

Coulomb blockade directional coupler

P. Pingue,^{a)} V. Piazza, and F. Beltram
 NEST-INFM & Scuola Normale Superiore, I-56126 Pisa, Italy

I. Farrer, D. A. Ritchie, and M. Pepper
 Cavendish Laboratory, University of Cambridge, Madingley Road, Cambridge CB3 0HE,
 United Kingdom

(Received 7 October 2004; accepted 16 December 2004; published online 26 January 2005)

A tunable directional coupler based on Coulomb blockade effect is presented. Two electron waveguides are coupled by a quantum dot to an injector waveguide. Electron confinement is obtained by surface Schottky gates on a single GaAs/AlGaAs heterojunction. Magneto-electrical measurements down to 350 mK are presented and large transconductance oscillations are reported on both outputs up to 4.2 K. Experimental results are interpreted in terms of Coulomb blockade effect and the relevance of the present design strategy for the implementation of an electronic multiplexer is underlined. © 2005 American Institute of Physics. [DOI: 10.1063/1.1857078]

Controlled directional injection of electrons from one electronic waveguide to another is being intensively investigated owing to its importance in wavelength multiplexing and in telecommunication routing devices. While photonic multiplexers represent a mature technology, electronic steering devices are still at their infancy.

Pioneering designs were demonstrated exploiting a field-effect tunable barrier between two semiconductor waveguides,^{1–5} implementing a Y-branch switch or switching the electrons by means of electric side-gates.^{6–8} An electronic device based on two electron waveguides coupled by an open interaction window rather than a tunneling barrier was also proposed^{9–11} and realized,¹² but so far no switching behavior has been demonstrated in this configuration.

In this letter we describe a scheme where the coupling element between two semiconductor waveguides is a single quantum dot (QD) and Coulomb blockade (CB) governs electron routing. We shall demonstrate that in the classic configuration with two electron waveguides mixing at an open ballistic window a QD can be induced—with appropriate biasing conditions and geometry—and employed as a gate-controlled coupling element between the two waveguides.

Figure 1(a) shows a scanning electron microscope (SEM) picture of the device. Schottky gates are labeled g1–g4. The Al split-gate structure was nanofabricated by e-beam lithography and thermal evaporation. The waveguides of the device described in this work have a total length $L = 7.5 \mu\text{m}$ each and a geometrical width $W = 0.44 \mu\text{m}$. The central split-gate is $w = 0.17 \mu\text{m}$ wide while the coupling window is $l = 0.57 \mu\text{m}$ long. The GaAs/AlGaAs heterostructure contains a two-dimensional electron gas (2DEG) located 70 nm below the surface with a mobility of $\mu = 3.7 \times 10^5 \text{ cm}^2/\text{Vs}$ and a carrier concentration of $n = 2.4 \times 10^{11} \text{ cm}^{-2}$ at 350 mK.

In our experiment gates g2–g4 were negatively biased by a dc voltage (V_{g2} , V_{g3} , V_{g4} , respectively), while gate g1 (biased V_{g1}) was employed as a plunger gate. A drain-source ac voltage ($V_{DS} = 100 \mu\text{V}$) was applied at the input waveguide (Ohmic contact D in Fig. 1).

The ac current flowing through outputs B and C was measured by two current preamplifiers and phase-locked techniques. A lower ac excitation of $20 \mu\text{V}$ was also used to test that the device was in the linear regime also at the lowest temperatures.

Panel (b) and (c) in Fig. 1 show the differential conductance measurements relative to collectors B and C, respectively, when an ac bias is applied to contact D. The Ohmic-contact A was left floating. Biasing V_{g2} , V_{g3} , and V_{g4} at -0.65 V , high-contrast oscillations in the output current appear on both collector waveguides at 350 mK as a function of V_{g1} in the range from -1.24 to -1.1 V . One of the outputs (Fig. 1, c) displays a 5%-wide current modulation while the

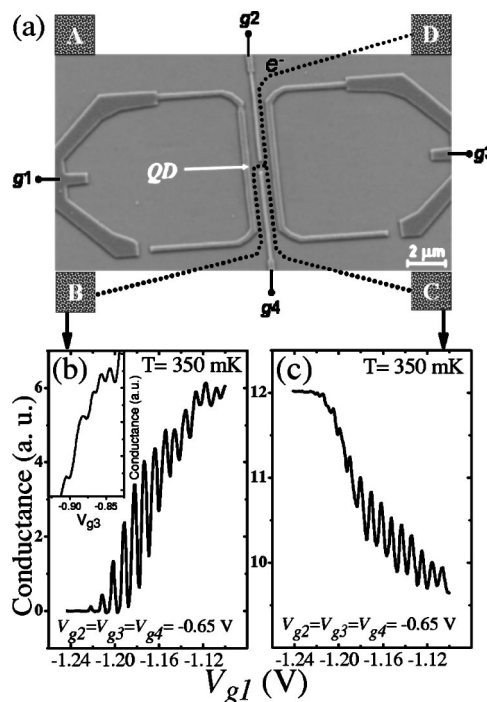


FIG. 1. (a) SEM picture of the coupled-waveguide device. Schottky gates are labeled as g1–g4. Letters A to D represent the Ohmic contacts (not shown); (b) differential conductance in the collector B (through the QD), and (c) corresponding conductance in the collector C. Inset: “symmetric dot” conductance as a function of V_{g3} .

^{a)}Electronic mail: pingue@sns.it

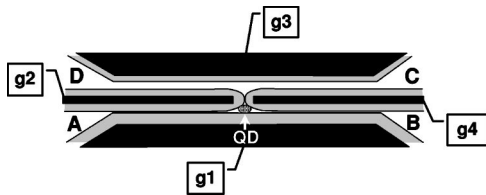


FIG. 2. Schematic of our device. QD indicates the quantum-dot location (black circle). Black regions represent the metal gates while gray areas show the regions depleted by the applied bias.

other collector (Fig. 1, b) shows a 100%-wide current modulation oscillation in the output current.

This behavior can be explained taking into account the formation of a QD in the CB regime in the region indicated by the black disk in the schematic sketch shown in Fig. 2. The QD presence in that position was verified in all cool-downs, and a specific characterization of each waveguide was performed in order to exclude the presence of unintentional dots in the input or output channels.^{13,14} By symmetrically reversing the biasing configuration of gate electrodes a dot symmetrically located in the opposite of the coupling region could be induced. This dot was indeed observed when contact B was employed as emitter and A and D as collector waveguides (A, D). In the case of the device shown here it yielded a lower contrast in conductance measurements [see inset in Fig. 1(b)]. We attribute this behavior to a different coupling regime to the reservoir, probably related to the tunnel barrier of the output channel.

The CB-oscillation pattern obtained by measuring the current from contacts B and C showed a π phase shift, excluding the possibility that the QD extends to the whole central region and demonstrating the switching behavior of our device.

Figure 2 shows a scheme of our device: gate-depleted regions in the 2DEG are indicated by gray areas. It is quite intuitive that a confined dot can be created when the coupling window is pinched-off and when the bottom waveguide is almost closed. Tunnel barriers originate from small grains or lithographic imperfections in the metallic gates that induce a constriction between the QD and the adjacent waveguides.

In the following, a low-temperature study of the magnetotransport properties of the dot represented in the scheme of Fig. 2 is reported. CB characterization was performed as a function of source-drain bias (V_{SD}) and as a function of a magnetic field parallel to the 2DEG plane, in order to minimize orbital magnetic-coupling effects. Figure 3(a) shows

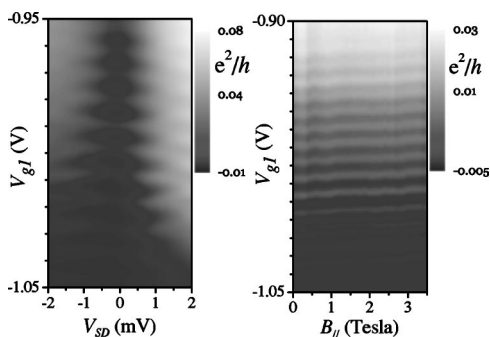


FIG. 3. Conductance behavior of the QD at finite bias (left panel) and in magnetic field parallel to the 2DEG (right panel). $T=350$ mK.

the well-known Coulomb diamonds in the QD conductance as a function of V_{SD} and V_{g1} . The height (in the V_{SD} direction) of the diamonds can be used to measure the charging energy U_{CB} between two adjacent electron levels.¹⁵ From the maximum Coulomb gap $U_{CB}=e^2/C_{tot}\approx 1.6$ meV a total dot capacitance of $C_{tot}\approx 100$ aF is deduced.

In a simple model of an ungated 2D disk-shaped QD the total capacitance is given by $C_{tot}=4\epsilon_0\epsilon_r D$, where D is the QD diameter, and $\epsilon_r=12.5$ is the dielectric constant of GaAs. From the measured value of $C_{tot}=100$ aF we derive a dot diameter of $D=0.23$ μm , in good agreement with the geometry of our device. From this diameter and the charge density of electrons in the original 2DEG, we estimate that there are ~ 100 electrons in the dot under the operating conditions of Fig. 3, left.

The mean periodicity of the Coulomb oscillations reported in Fig. 1 $\Delta V_{g1}=e/C_{g1}=9.4$ mV corresponds to a gate capacitance of $C_{g1}=17$ aF giving, therefore, $\eta=C_{g1}/C_{tot}=0.17$ as “lever arm” value between the applied gate voltage and the change in the total energy of the island. The period ΔV_{g1} remains almost constant changing V_{g1} down to the pinch-off and no contribution related to discrete energy levels of the dot is observed. In any case, the pinch-off in our device is determined by that relative to the output channel QD-B, so no information about the occupation number of the dot is directly available through these measurements.

More information about the QD position can be extracted by comparing CB oscillations as a function of V_{g1} at different voltages applied to the remaining gates. We observed an increase of C_{g1} from 16.3 to 19 aF while decreasing V_{g2} , V_{g3} , and V_{g4} from -0.6 to -0.8 V, indicating that electrons in the dot are pushed toward g1 when the other gates are biased with increasingly negative voltages.

Measurements in parallel magnetic field B_{\parallel} (Fig. 3, right) show a common shift of the CB peaks that is caused by the coupling between the magnetic field itself and the transverse components of electron wave functions in the dot and in the leads (diamagnetic shift).^{16,17} By plotting the peak spacing in order to eliminate common peak motion with magnetic field and to minimize the presence of switching noise, a strong fluctuation in the data is observed (data not shown). The peak spacing does not follow a clear linear behavior with the magnetic field as $g\mu_B B_{\parallel}/\eta$ (where g is the Landé factor for bulk GaAs, μ_B the Bohr magneton, and η the lever arm value) as expected on the basis of Zeeman splitting of the dot levels. This irregular behavior has been already observed in gate-depleted QDs in the “weak-coupling” regime:^{18,19} the QD is indeed weakly coupled to drain and source and CB peaks typically have a height lower than $0.1 e^2/h$ (see Fig. 3, right) and an irregular pattern of the peak spacing in function of the magnetic field is reported.

Finally, the temperature behavior of our device (see Fig. 4) shows that the effect is still present up to 4.2 K, consistent with the CB charging energy U_{CB} previously found.

We wish to point out an advantage intrinsic to this scheme with respect to quantum devices based on coherence effects: as for the case of single electron transistors,^{20,21} appropriate geometries and materials can lead to higher and even room-temperature operation of such CB-based directional coupler. Available transconductance values are very high. In fact at low temperatures switching voltages are in the millivolt range and at least one order of magnitude lower than those required in Y-branch devices (operated both in the

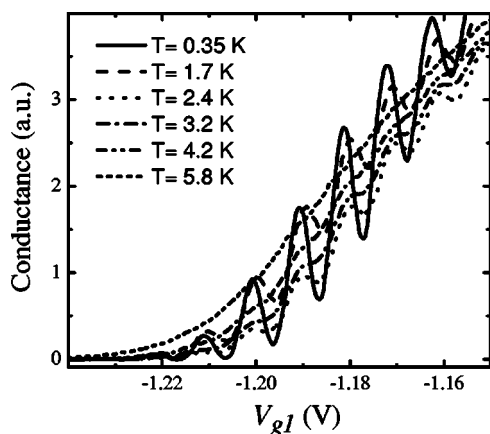


FIG. 4. Temperature behavior of the CB effect in the collector B: conductance oscillations are present from 0.35 up to 4.2 K.

so-called “external side-gate”⁷ and in “internal ballistic” switching mode⁸). This leads to measured normalized-transconductance values as high as $I^{-1}dI/dV_{g1} \sim 1500 \text{ V}^{-1}$ for collector B in the present implementation. This characteristic is of interest in terms of low power consumption for high miniaturization and large scale integration.

In conclusion, a directional coupler device based on CB was demonstrated. Its differential-conductance characterization as a function of magnetic field and temperature was presented. In the CB regime this device behaves like a current switch in one collector output and as a current modulator in the opposite one. The same basic scheme can be employed to design logic functions or, employing a series of our device, a CB-based electronic multiplexer.

Fruitful discussions with S. de Franceschi and M. Governale are gratefully acknowledged. This work was supported in part by the European Research and Training Net-

work COLLECT (Project No. HPRN-CT-2002-00291). Work at NEST-INFM was supported in part by MIUR under FIRB Contract No. RBNE01FSWY, and work at Cavendish Laboratory by EPSRC.

- ¹J. A. del Alamo and C. C. Eugster, *Appl. Phys. Lett.* **56**, 78 (1990).
- ²C. C. Eugster and J. A. del Alamo, *Phys. Rev. Lett.* **67**, 3586 (1991).
- ³C. C. Eugster, J. A. del Alamo, M. J. Rooks, and M. R. Melloch, *Appl. Phys. Lett.* **64**, 3157 (1994).
- ⁴N. Tsukada, A. D. Wieck, and K. Ploog, *Appl. Phys. Lett.* **56**, 2527 (1990).
- ⁵N. Tsukada, M. Gotoda, M. Nunoshita, and T. Nishino, *Phys. Rev. B* **53**, R7603 (1996).
- ⁶T. Palm and L. Thylen, *Appl. Phys. Lett.* **60**, 237 (1992).
- ⁷L. Worschech, B. Weidner, S. Reitzenstein, and A. Forchel, *Appl. Phys. Lett.* **78**, 3325 (2001).
- ⁸K. Hieke and M. Ulfward, *Phys. Rev. B* **62**, 16727 (2000).
- ⁹J. Wang, H. Guo, and R. Harris, *Appl. Phys. Lett.* **59**, 3075 (1991).
- ¹⁰O. Vanbésien and D. Lippens, *Appl. Phys. Lett.* **65**, 2439 (1994).
- ¹¹Y. Takagaki and K. Ploog, *Phys. Rev. B* **49**, 1782 (1994).
- ¹²Y. Hirayama, A. D. Wieck, T. Bever, K. von Klitzing, and K. Ploog, *Phys. Rev. B* **46**, 4035 (1992).
- ¹³H. van Houten and C. W. J. Beenakker, *Phys. Rev. Lett.* **63**, 1893 (1989).
- ¹⁴A. A. M. Staring, H. van Houten, C. W. Beenakker, and C. T. Foxon, *Phys. Rev. B* **45**, 9222 (1992).
- ¹⁵L. P. Kouwenhoven, C. M. Marcus, P. L. McEuen, S. Tarucha, R. M. Westervelt, and N. S. Wingreen, in *Mesoscopic Electron Transport*, edited by L. L. Sohn, L. P. Kouwenhoven, and G. Schön (Kluwer, Dordrecht, 1997), Vol. 345, p. 105.
- ¹⁶J. Weis, R. J. Haug, K. V. Klitzing, and K. Ploog, *Phys. Rev. Lett.* **71**, 4019 (1993).
- ¹⁷D. S. Duncan, D. Goldhaber-Gordon, R. M. Westervelt, K. D. Maranowski, and A. C. Gossard, *Appl. Phys. Lett.* **77**, 2183 (2000).
- ¹⁸J. A. Folk, C. M. Marcus, R. Berkovits, I. L. Kurland, I. L. Aleiner, and B. L. Altshuler, *Phys. Scr.* **90**, 26 (2001).
- ¹⁹S. Lindemann, T. Ihn, T. Heinzl, W. Zwerger, K. Ensslin, K. Maranowski, and A. C. Gossard, *Phys. Rev. B* **66**, 195314 (2002).
- ²⁰T. A. Fulton and G. J. Dolan, *Phys. Rev. Lett.* **59**, 109 (1987).
- ²¹J. Shirakashi, K. Matsumoto, N. Miura, and M. Konagai, *Appl. Phys. Lett.* **72**, 1893 (1998).